could only afford to calculate $\Delta\alpha(\omega)$ three times]; (ii) our main interest was in explaining the principal physical features of the spectra which are caused by excitons; (iii) an extremely precise fit to the data requires a knowledge of the effects of nonuniform fields, energy-dependent broadening, and bandwarping—to some extent these effects afford the fitting procedure with additional parameters for optimizing the agreement between experiment and theory without any confidence that these optimal values of the fitting parameters are physically realistic. For example, in our fit with the Si data (Fig. 7), we could increase the agreement on the high-energy side of the spectrum by reducing the value of Γ by about 50%. This would cause the theoretical curve to be too large in the bound-exciton region, a situation which could be fixed by judiciously altering the transition matrix element, the reduced effective mass, and the field inhomogeneity. However, such a procedure tends to obscure the underlying physics and should be avoided; furthermore, we believe that there is a physical reason for the discrepancy between theory and experiment at high energy. This discrepancy will be discussed later in Sec. V.

[26]Note that we have $f = |e|Fa/R \propto \mu^{-2}$ and $R \propto \mu$. The fitting procedure determines f and R, but only approximately, so that variation of f may be ascribed to variation of F or m or both.

[27]In Ge, the light and heavy holes have masses of $0.04\,m_0$ and $0.3m_0$, respectively. [See C. Kittel, *Introduction to Solid State Physics*, 3rd ed. (Wiley, New York, 1966), p. 322.] The average conduction band mass is $0.263m_0$. Thus the total masses and the reduced masses are $0.3m_0$ and $0.035m_0$ for the light-hole band and $0.563m_0$ and $0.14m_0$ for the heavy-hole band. The corresponding numbers (Ref. 2) for Si are $0.16m_0$, $0.49m_0$, $0.26m_0$, $0.42\,m_0$, $0.10m_0$, $0.75m_0$, and $0.17m_0$, respectively. Near $E=0$, the indirect absorption coefficient varies nearly as $\mu^2M^{3/2}$. Thus we have $[\mu^2M^{3/2}\ (\text{light})]/[\mu^2M^{3/2}\ (\text{heavy})]$ equal to 0.024 and 0.15.

[28]The high-energy side of the first peak of $\Delta\alpha(\omega)$ is steeper than the low-energy side. Thus, when the peak is broadened, it generally moves to lower energy.

[29]An additional differentiation of $\Delta\alpha(\omega)$ (with respect to, say, photon wavelength) would probably exhibit the broadened $2s$ state dramatically.

[30]D. Long, *Energy Bands in Semiconductors* (Wiley, New York, 1968), p. 163.

[31]D. E. Aspnes and A. Frova, Solid State Commun. 7, 155 (1969).

[32]This can be seen by noting that $\Delta\alpha(\omega, F)$ for energies well above E_{gap} is (in the one-electron approximation) from the Appendix

$$\Delta\alpha(\omega) = \tilde{D}_v\left(\frac{2M_v}{\hbar^2}\right)^{3/2}(32\pi a^3R^{3/2})^{-1}E_0^2[A\xi^{-9/4}\sin(\tfrac{2}{3}\xi^{3/2}+\tfrac{1}{4}\pi) - B\xi^{-15/4}\cos(\tfrac{2}{3}\xi^{3/2}+\tfrac{1}{4}\pi)+O(\xi^{-21/4})],$$

where A and B are constants, $\xi = E_0/[R(\frac{1}{2}f)^{2/3}]$, and $E_0 = \hbar\omega \mp \hbar\Omega_{\vec{K}m} - E_{\text{gap}}$. In contrast, the derivative is

$$F\frac{\partial}{\partial F}\alpha(\omega, F) = \tfrac{3}{2}\Delta\alpha(\omega) - \tilde{D}_v\left(\frac{2M}{\hbar^2}\right)^{3/2}(32\pi a^3R^{3/2})^{-1}E_0^2 \times[(\tfrac{2}{3}A\xi^{-3/4}+B\xi^{-15/4})\cos(\tfrac{2}{3}\xi^{3/2}+\tfrac{1}{4}\pi) + \tfrac{2}{3}B\xi^{-9/4}\sin(\tfrac{2}{3}\xi^{3/2}+\tfrac{1}{4}\pi)].$$

Note that for high energies the term with $\xi^{-3/4}$ is larger than the dominant term in $\Delta\alpha(\omega, F)$ which only goes as $\xi^{-9/4}$.

PHYSICAL REVIEW B VOLUME 4, NUMBER 12 15 DECEMBER 1971

Electron-Tunneling Studies of a Quantized Surface Accumulation Layer

D. C. Tsui
Bell Telephone Laboratories, Murray Hill, New Jersey 07974
(Received 22 July 1971)

This paper describes an experiment on electron tunneling through n-type InAs-oxide-Pb junctions and discusses in detail two results which are pertinent to the quantization of an accumulation layer at the InAs surface. First, the tunneling curves dI/dV vs V and d^2I/dV^2 vs V show structures reflecting the energy minima of two-dimensional electric subbands. The bias position of these structures gives a direct measure of the energy of the quantized levels. Second, when a quantizing magnetic field is applied perpendicular to the junction surface, oscillations are observed in the tunneling curves. These oscillations reflect the Landau-level spectra of electrons in the electric subbands. They give a direct measure of the effective mass of the surface electrons.

I. INTRODUCTION

In an accumulation or inversion layer of a semiconductor surface, if the electric field associated with the surface layer is sufficiently strong, the energy due to a carrier's motion normal to the surface is quantized into discrete levels. Since a continuum of energy is allowed for motion parallel to the surface, the energy structure of the surface carrier is a series of two-dimensional bands called electric subbands, each corresponding to a quantized level. The existence of these two-dimensional conducting states, predicted by Schrieffer,[1] was experimentally confirmed by Fowler *et al.*[2] several years ago using surface magnetoresistance measurements on the n-type inversion layer of a {100} sili-

con surface. Since then, surface quantization effects have been observed in the transport properties of n-type inversion layers on Si, InAs, InSb, and $Hg_{1-x}Cd_xTe$ single crystals.[3-8]

In the case of a surface accumulation layer, conventional transport measurements have not yielded similar information concerning surface quantization effects. Only recently, quantization of the surface accumulation layer at an n-type InAs-oxide interface was observed using electron-tunneling techniques.[9] The existence of an accumulation layer at the real surface of an n-type InAs crystal has been known for some years from studies of electron transport through metal-semiconductor contacts[10] and of photoemission phenomena.[11]

This paper describes the experiments on electron tunneling through n-type InAs-oxide-Pb junctions and discusses in detail two results which are pertinent to the quantization of a surface accumulation layer. First, the tunneling curves, i.e., the conductance (dI/dV) versus bias (V) curves and the derivative of the conductance (d^2I/dV^2) versus V curves, show structures reflecting the energy minima of the two-dimensional electric subbands. The bias position of these structures gives a direct measure of the energy of the quantized levels. Second, when a quantizing magnetic field is applied perpendicular to the junction surface (i.e., parallel to the tunnel current direction), oscillations are observed in the tunneling curves. These oscillations reflect the Landau-level spectra of electrons in the electric subbands. They give a direct measure of the effective mass of the surface electrons.

II. THEORETICAL MODELS

A. Quantization of InAs Surface Accumulation Layer

Figure 1 shows the potential energy diagram of an idealized InAs-oxide-Pb tunnel junction at zero bias. E_c is the conduction-band edge of bulk InAs and μ is its Fermi level. We choose the z axis

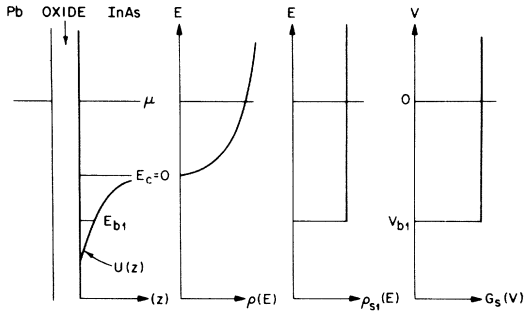

FIG. 1. Potential-energy diagram of an n-type InAs-oxide-Pb junction at zero bias, the density of states $\rho(E)$ of the conduction band, the density of states $\rho_{s1}(E)$ of a subband, and the tunnel conductance $G_s(V)$ vs V due to the subband electrons.

normal to the junction surface and measure energy from E_c (energy above E_c is positive). The main feature is that the InAs conduction band bends downward at the surface and forms a one-dimensional potential well $U(z)$, whose width is comparable to the de Broglie wavelength of the electrons in the conduction band.

This band bending results from redistribution of conduction electrons near the surface to screen out an external electric field, which probably has its origin in the defects of the oxide layer. The potential energy $U(z)$ is determined by the electronic charge distribution through Poisson's equation

$$d^2U(z)/dz^2 = -4\pi e\rho(z)/\kappa \ , \tag{1a}$$

with boundary conditions

$$U(\infty) = 0 \ , \tag{1b}$$

$$\left.\frac{-dU(z)}{dz}\right|_{z=0} = eF_0 \ . \tag{1c}$$

Here $\rho(z)$ is the charge density given by the surface electrons, the bulk conduction-band electrons, and the donor impurities. F_0 is the external electric field at the InAs-oxide interface $z = 0$. Since the electron distribution must be determined quantum mechanically by solving Schrödinger's equation of the crystal with the surface potential $U(z)$, a simultaneous solution of both Schrödinger's and Poisson's equations is required to determine $U(z)$.

Stern and Howard[12] have given a self-consistent calculation for an n-type inversion layer of Si when one quantum level is involved. In that case, there are no bulk conduction-band electrons and the parabolic description of the conduction band is adequate. Recently, Appelbaum and Baraff[13] have developed a scheme for making self-consistent calculations on the quantum state of a surface accumulation layer with a parabolic energy band. In order to clarify some basic physical concepts, which are necessary to understand our experimental results, we shall ignore the problem of self-consistency and of the nonparabolic nature of the energy band in discussing the quantization of the surface accumulation layer. We regard the conduction electron as a particle with mass m^* in a box and study its energy structure when a potential well $U(z)$ is introduced at an edge of the box.

Before $U(z)$ is introduced, the energy of the particle is given by

$$E = (\hbar^2/2m^*)(k_x^2 + k_y^2 + k_z^2) \ , \tag{2}$$

where k_x, k_y, and k_z are the x, y, and z components of its wave vector. The energy associated with the z component of its motion is $E_z = (\hbar^2/2m^*)k_z^2$. The introduction of $U(z)$ modifies the z component of the particle motion and alters its energy structure according to

$$(-\hbar^2/2m^*)[d^2\varphi(z)/dz^2]+U(z)\varphi(z)=E_z\varphi(z)\,. \tag{3}$$

Since $U(z)$ is an attractive potential well, E_z can be either positive, in which case a continuum of values is allowed, or negative, in which case only discrete values are allowed. For $E_z>0$, $\varphi(z)$ is a propagating wave and the energy of the electron is given by Eq. (2). We refer to electrons in these states as bulk conduction electrons. For $E_z<0$, however, $\varphi(z)$ is a bound state denoted by a quantum number n; that is, the wave function is concentrated inside the potential well. Since the energy for motion along the surface is not altered by $U(z)$, these electric-field-induced surface states form a series of two-dimensional energy bands given by

$$E_n=E_{bn}+(\hbar^2/2m^*)\,(k_x^2+k_y^2). \tag{4}$$

The energy minima of these two-dimensional bands are at the binding energy of the quantized levels, E_{bn}. Following Stern and Howard, we shall call these energy bands electric subbands and refer to the electrons occupying these states as surface electrons.

Duke[14] obtained analytic solutions of Eq. (3) for $U(z)=-U_0e^{-z/z_0}$ and $U(0)=\infty$. In this exponential form, the surface potential well is parametrized by a surface potential U_0 and a characteristic field penetration length z_0. The energy of the quantized levels is then given by

$$E_b=\hbar^2p^2/8m^*z_0^2\,, \tag{5a}$$

where p is determined by the Bessel-function relation

$$J_p(q)=0,\quad q=(8m^*U_0z_0^2/\hbar^2)^{1/2}. \tag{5b}$$

We shall make a comparison of our experimental data with this simple model in Sec. IV.

B. Tunneling of Surface Electrons

If the bound-state wave function $\varphi(z)$ of the surface electrons is allowed to penetrate into the oxide and to overlap with the wave function of the metal electrode, electron tunneling occurs. When a bias V is applied to the metal electrode, the tunnel current due to electrons in the nth subband is given by

$$J_{sn}(V)\propto\int_{\mu-eV}^{\mu}d\epsilon\,\rho_{sn}(1/\tau_n)\,, \tag{6}$$

where $1/\tau_n$ is the electron-tunneling probability per unit time and ρ_{sn} is the electron density of states of the nth subband. Since all the electrons in a given subband E_n have the same bound-state wave function $\varphi_n(z)$, the tunneling probability is independent of energy. We neglect the effect of bias on the oxide barrier and on the surface potential well $U(z)$. Then, the tunnel conductance due to electrons of the nth subband, $G_{sn}(V)\equiv\partial J_{sn}(V)/\partial V$, is proportional to ρ_{sn}. This result was first given by BenDaniel and Duke.[15]

We assume the conduction band of InAs parabolic in Fig. 1. The density of states of the subband is constant and has a step discontinuity at its energy minimum E_{b1}. The total conductance of the junction will therefore show a sudden decrease in the Pb(+) bias when the Fermi level of Pb is aligned with the energy level E_{b1}. The bias, at which the decrease occurs, is a measure of E_{b1} with respect to the Fermi energy of the bulk sample.

We have neglected the effects of an applied bias on $U(z)$. We assumed that the electric field from the bias goes to zero at the interface $z=0$ and, therefore, the potential difference between the two electrodes is taken up entirely by the oxide layer. This assumption is obviously inadequate when the oxide thickness is comparable to or less than the characteristic length of the electric field penetration into the InAs electrode. For then, an appreciable fraction of the total potential difference drops across the InAs electrode. The exact amount is a sensitive function of the oxide properties and must be determined by a simultaneous solution of Schrödinger's and Poisson's equations.[16]

We shall not attempt any estimate of these effects for lack of definite information concerning the oxide properties. We shall instead illustrate a qualitative effect of the bias on the over-all shape of the junction-conductance-versus-bias curve. This is shown in Fig. 2. At zero bias, the band bending at $z=0$ is U_0. The barrier height at $z=0$ seen by electrons at the InAs Fermi level is given by

$$\phi_1=\chi-(U_0+\mu)\,, \tag{7}$$

where χ is the electron affinity at the surface[17] and μ is the Fermi energy of the bulk conduction electrons. If a positive bias V is applied to the Pb electrode, additional electrons must accumulate at the surface to screen out the electric field from the applied bias. Since the Fermi level is fixed with respect to the energy minimum of the bulk

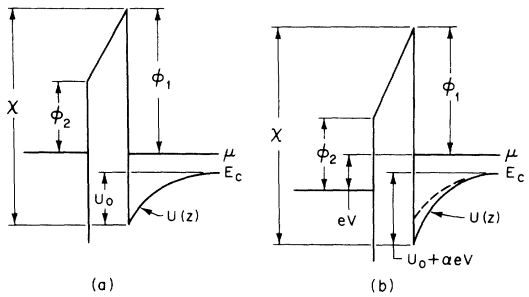

FIG. 2. Idealized potential-energy diagram of an n-type InAs-oxide-Pb junction: (a) at zero bias and (b) with a bias V applied to the Pb (left-hand side) electrode.

conduction band, $U(z)$ must be modified to accommodate the additional electrons. If a fraction α of the applied potential drops across the InAs electrode, the band bending at the surface will increase by αeV and the barrier height ϕ_1 will decrease by αeV. Similarly, if a negative bias is applied to the Pb electrode, ϕ_1 will increase by the amount of the bias potential which is dropped across the InAs. Consequently, an applied bias enhances tunneling of electrons out of the InAs electrode and suppresses tunneling of electrons into it. This effect will make the conductance-versus-bias curve of the junction asymmetric.

C. Landau Levels

When a magnetic field is applied normal to the junction surface, it leads to a complete quantization of the energy of electrons in a subband. Consequently, the electron density of states ρ_s of the subband is a series of δ-function peaks at the energy of the Landau levels. The tunnel conductance due to the subband electrons is proportional to ρ_s and reflects these Landau-level peaks. However, because of level broadening, these peaks will be rounded off and appear as oscillations in the dI/dV-vs-V and d^2I/dV^2-vs-V curves of the junction. The period of the oscillations gives a measure of the Landau-level separation.

Stern and Howard[12] have calculated the energy of an electron in the ground-state subband in the presence of an arbitrarily oriented magnetic field and it is given by

$$E = E_b + \hbar\omega_c\,(l+\tfrac{1}{2}) + (e^2H_{xy}^2/2m^*c^2) \times[\langle z^2\rangle - \langle z\rangle^2]\ , \quad (8a)$$

$$\omega_c = eH_z/m^*c\ . \quad (8b)$$

Here, l is the Landau-level quantum number and H_z is the magnetic field component perpendicular to the surface. The unique characteristic of a two-dimensional electron gas is that its cyclotron frequency ω_c depends only on H_z. $\langle z\rangle$ and $\langle z^2\rangle$ are the values of z and z^2 averaged over the ground-state wave function. The parallel component of the magnetic field, H_{xy}, gives rise to a small shift of the energy minimum of the subband. This shift, which varies quadratically with H_{xy}, has recently been observed.[18]

III. EXPERIMENTAL DETAILS

A. Sample Preparation

The tunnel junctions are fabricated on bulk n-type single-crystal InAs samples, which are usually $8\times5\times1$-mm platelets. The sample surface is prepared by first mechanically polishing it to an optical finish and then chemically etching it in a solution of 1 part water, 1 part superoxol (30% hydrogen peroxide), and 3 parts concentrated sulfuric acid. The resulting surface is optically smooth and free of observable scratches. The sample is then outgased at 150 °C in a vacuum of 1×10^{-7} mm Hg for about 2 h. The oxide is grown at about 120 °C in a dry oxygen atmosphere for about 30 h.

The oxidized surface is then insulated by collodion except for a narrow strip in the middle. Cross strips of Pb about 2000 Å thick were evaporated on the sample in a vacuum of 2×10^{-6} mm Hg. Pure indium is used to solder gold wire leads to the Pb films and to the InAs sample. We use the standard cross-strip configuration to facilitate four terminal measurements.[19]

The quality of the junction is evaluated following the standard procedure used for evaluating superconducting tunnel junctions.[19,20] We have made detailed measurements on junctions which have room-temperature resistances varying from 50 to 1000 Ω. Junctions having higher resistance are usually too noisy to allow derivative measurements. The junction resistivity ratio $R(4.2\,^\circ\mathrm{K})/R(300\,^\circ\mathrm{K})$ is about 1.3 for all the junctions which proved to be tunnel junctions. At 1 °K, the I-V, dI/dV-vs-V, and d^2I/dV^2-vs-V curves of all these junctions show the superconducting Pb energy gap and the Pb-phonon-induced structure in the superconducting tunneling density of states which are in quantitative[20] agreement with those measured on high-quality Al-oxide-Pb junctions. We shall discuss only the data taken from these junctions.

B. Measuring Techniques

The measurements to be made are the first and second derivatives of the junction I-V characteristic as a function of V and as a function of the magnetic field H. The method for taking derivatives is the standard harmonic detection of an applied ac modulation signal using a phase-sensitive detector. The circuits used in this work have previously been discussed in detail by McMillan and Rowell[20] and by Thomas and Rowell.[21] We use a modulation frequency of 500 Hz. dV/dI is measured directly by detecting the ac signal at the fundamental frequency. The ac signal detected at the second harmonic is proportional to the d^2I/dV^2. The proportionality constant, however, contains the junction impedance as a factor. This factor does not vary drastically over the bias range we have studied. We shall refer to this second-harmonic signal as the directly measured d^2I/dV^2. We also record the dV/dI-vs-V data digitally and compute dI/dV vs V and d^2I/dV^2 vs V numerically.[22] We shall refer to these curves as the conductance-versus-bias and the d^2I/dV^2-vs-V curves.

The magnetic field is generated by a 1-in.-bore Nb_3Sn superconducting solenoid and measured by a copper magnetoresistance probe[23] mounted directly on the sample holder. The stability of the mag-

net allows a 2% accuracy for field measurements above 40 kG and a 4% accuracy for field measurements from 15 to 40 kG. A rotating sample holder is used so that the tunnel junctions can be rotated 180° about an axis normal to the magnetic field direction.

IV. RESULTS AND DISCUSSIONS

In this section, we shall discuss the results from our tunneling measurements on n-type InAs-oxide-Pb junctions which are pertinent to quantization of the accumulation layer at the InAs surface. The data are taken at 4.2 °K and they show no temperature dependence as the tunnel junctions are cooled from 4.2 to 1 °K. We obtain these normal-state data by applying a magnetic field ($H \approx 2$ kG) perpendicular to the junction surface to quench the Pb superconductivity. We shall adopt the convention that the InAs electrode is at ground potential and that the bias is the voltage applied to the Pb electrode.

A. Quantized Energy Levels

We summarize in Table I our results which are pertinent to the quantum state energy levels of the InAs surface accumulation layer. N is the electron concentration of the bulk sample determined from Hall-effect measurements at 4.2 °K. The Fermi energy E_F is calculated from N using the two-band model: $E(1+E/E_g)=(\hbar^2/2m_0^*)k^2$, evaluated at $k_F = (3\pi^2N)^{1/3}$ with a band-edge mass $m_0^* = 0.021m$ and a band-gap energy $E_g = 0.41$ eV.[24] V_{b1} and V_{b2} are the biases at which structures in the tunneling curves due to the quantized levels are observed. We shall discuss these structures in detail in the following paragraphs.

Figure 3 shows the normal-state tunnel conductance versus bias curve measured on junction 311 of sample 5770 in Table I. As bias increases, the conductance increases faster in the Pb(+) polarity than in the Pb(−) polarity. We have observed this asymmetry in the conductance-versus-bias curves

TABLE I. A summary of results pertinent to the energy levels of the InAs surface accumulation layer.

Sample No.	Orientation	N (cm^{-3})	E_F (meV)	Junction No.	V_c (mV)	V_{b1} (mV)	V_{b2} (mV)
1811		1.6×10^{18}	168	212	154	201	
1840	{111}	1.6×10^{18}	168	212	158	255	
57891	{111}	5.5×10^{17}	95	212	98	183	
57892	{111}	4.5×10^{17}	85	68	93	195	
				59	93	200	
				212	90	185	
57893	{111}	4.5×10^{17}	85	59	98	192	
57894		5.4×10^{17}	95	212	97	168	
5770	{111}	5.4×10^{17}	95	311	97	198	
				59	97	195	
5751	{111}	5.4×10^{17}	95	212	100	225	
				410	100	225	
5711	{111}	5.4×10^{17}	95	212	100	212	
				311	100	210	
				410	100	230	
5740	{110}	5.4×10^{17}	95	410	98	235	
5780	{110}	5.4×10^{17}	95	410	100	255	
				59	100	255	
5741	{100}	5.4×10^{17}	95	410	97	195	
				311	95	200	
17101	{111}	1.5×10^{17}	44	212	60	168	
				311	58	142	
17102	{111}	1.5×10^{17}	44	212	55	130	
				311	55	130	
1740	{111}	1.5×10^{17}	44	59	53	80	138
2679P	{111}	2.2×10^{16}	13	212	18	52	172
				311	20	52	175
2689P		2.2×10^{16}	13	212	26	72	225
				311	26	74	229
				410	25	70	220
2640	{111}	2.2×10^{16}	13	311	25	74	232
26120		2.2×10^{16}	13	68	18	50	173
				59	18	48	163
				311	18	50	172

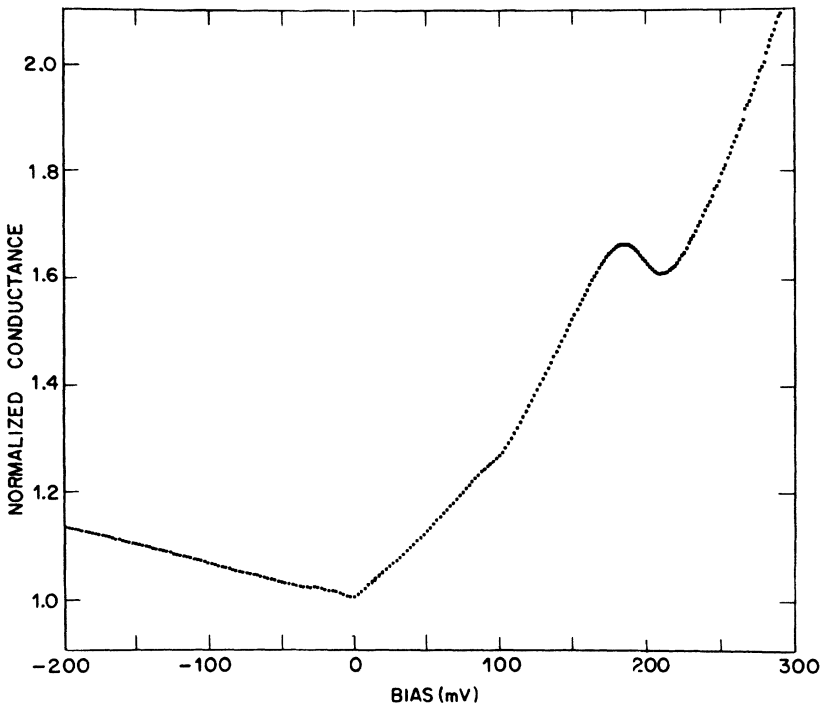

FIG. 3. Normalized conductance $(dI/dV)/(dI/dV)_{V=0}$ versus bias curve measured on junction 311 of sample 5770 in Table I. $T = 4.2$ °K, $H \approx 2$ kG. The bias is the voltage applied to the Pb electrode.

of all the junctions. This observation is in qualitative agreement with the effect of an applied bias on $U(z)$ which was discussed in Sec. II B.

The fine structures near zero bias ($|V| \lesssim 30$ mV) are due to emission and self-energy effects of Pb phonons and InAs phonons. These effects have been discussed previously.[22,25] The structure at $V \simeq +100$ mV is due to the cutoff of the conduction-electron density of states at the InAs conduction-band minimum. The bias position V_c of this structure is a direct measure of the Fermi energy of the conduction-band electrons. The Fermi energy E_F calculated from the electron concentration N using the two-band model is in fair agreement with this tunneling result.[26]

The sudden decrease in conductance at $V \approx +200$ mV is due to a quantized energy level in the surface potential well of the InAs accumulation layer. In the d^2I/dV^2-vs-V curve (Fig. 5) this structure appears as a dip. The bias position of this dip ($V = +198$ mV), which corresponds to the steepest decrease in conductance, is a measure of the energy of the quantized level relative to the InAs Fermi level. We use V_{b1} to designate this bias position. The binding energy E_{b1} of the surface electrons is given by $E_{b1} = eV_{b1} - E_F$.

The width of this dip at half its minimum depth is analogous to the half-width of a spectral line. It is a direct measure of the energy broadening of the quantum level. However, we have observed that this half-width varies from sample to sample even for samples which have the same bulk properties. For example, a half-width varying from 25 to 45 mV is obtained from junctions fabricated on various samples, all of which have $N = 5.5 \times 10^{17}/\text{cm}^3$ and μ_N(mobility) = 16 000 cm^2/V sec. This observation suggests that the measured half-width is due to the inhomogeneity of the electric field which gives rise to the surface potential well at the InAs-oxide interface.

We should note that eV_{b1} is obtained by applying a bias V_{b1} to the Pb electrode of the tunnel junction. The electric field due to V_{b1} can penetrate into the InAs electrode and modify the surface potential well $U(z)$ of the accumulation layer. Therefore, eV_{b1}, which measures the quantum state energy of the accumulation layer when a bias V_{b1} is applied to the Pb electrode, may differ from the quantum state energy of the accumulation layer with zero bias across the junction. We shall make no attempt to estimate this difference here.

The qualitative features of the conductance-versus-bias curve shown in Fig. 3 are representative of all the tunnel junctions fabricated on the more heavily doped samples ($n \gtrsim 1.5 \times 10^{17}/\text{cm}^3$). For these junctions, no conductance structure attributable to another subband minimum has been observed with bias up to $V \approx +400$ mV. We may also infer from the magneto-oscillatory effects, which will be discussed in Sec. IV B, that there are no quantized levels at an energy further below the InAs Fermi energy. This is based on the fact that we have not observed oscillatory effects due to Landau levels of another electric subband with magnetic

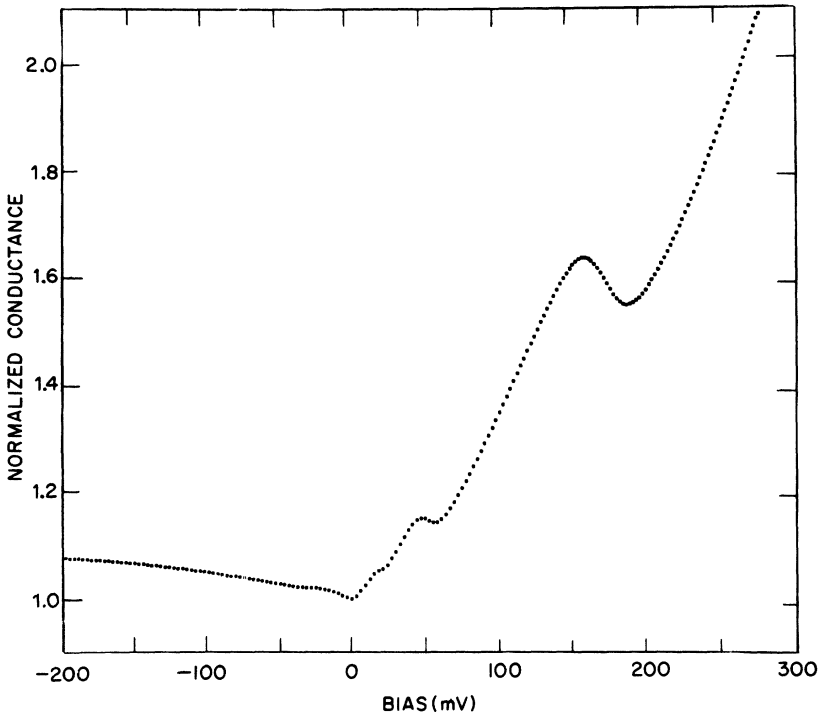

FIG. 4. Normalized-conductance-versus-bias curve measured on junction 212 of sample 2689P in Table I. $T = 4.2$ °K, $H \approx 2$ kG.

field strengths up to 100 kG. Therefore, we believe that there is only one quantized energy level in the surface potential well of these more heavily doped samples. The bias V_{b1} given in Table I is a measure of the ground-state energy of the quantized surface accumulation layer.

Figure 4 shows the conductance-versus-bias curve measured on junction 212 of sample 2679P in Table I. Its d^2I/dV^2-vs-V curve in the Pb(+) bias is shown as curve (b) in Fig. 5. The qualitative features of these tunneling curves, which are typical of all the junctions fabricated on samples having $N \lesssim 1.5 \times 10^{17}/\text{cm}^3$, show structures due to two quantized levels. These are the sudden decrease in conductance at $V = +52$ mV and at $V = +172$ mV. The structure at $V = +18$ mV is a reflection of the conduction-band minimum. As pointed out in an earlier paper, [25] the structure due to the ground-state level is much stronger than that due to the excited-state level. This is understandable because the tunneling probability of electrons in the subbands increases with increasing bias. Since the structure due to the ground-state level is observed at a much larger bias, it is expected to be stronger than that due to the excited-state level. On the other hand, since the electron decay length in a tunnel barrier is determined by the electronic properties of the insulating layer, the variation of effective mass in the InAs conduction band cannot account for this result. Also, it seems unnecessary to invoke the mechanism that electrons tunnel through the oxide valence band to explain this result. [25]

Table I shows that the surface electron binding energy ($E_b = eV_b - eV_c$) obtained from junctions which are fabricated on different samples having the same bulk electron concentration, or from junctions fabricated at different times on the same sample, can differ by as much as 40%. On the other hand, E_b

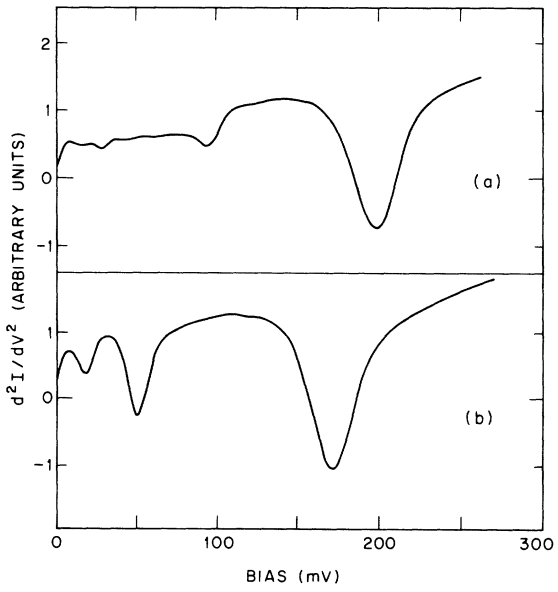

FIG. 5. d^2I/dV^2-vs-V curves of (a) junction 311 of sample 5770 and (b) junction 212 of sample 2679P.

obtained from different junctions fabricated at the same time and on the same sample do not differ by more than 10%. This qualitative result suggests that the electric field at the interface, which gives rise to the accumulation layer, is extremely sensitive to the properties of the oxide in proximity. In fact, it is indicative that this electric field may have its origin in the oxide defects. However, we have not been able to eliminate the work-function difference between the electrodes as another important origin. We have also observed that E_b obtained from samples having {110} oriented surface is consistently larger than E_b obtained from samples having {111} or {100} oriented surface. We should note that in an InAs crystal the number of atoms per unit area is denser in a {110} plane than in either a {111} plane or a {100} plane.[27]

The surface potential well $U(z)$ of the accumulation layer is determined by the electric field at the interface $z=0$ and the static screening of the electrons near the surface. We have seen that the electric field at $z=0$ is extremely sensitive to the oxide in proximity. Despite the fact that we have not been able to control the oxide properties, we have demonstrated that $U(z)$ can indeed be varied by varying the Fermi degeneracy of the bulk sample. This is implicit in our result that the samples with $N<1.5\times10^{17}/\mathrm{cm}^3$ always have two quantized levels in the surface potential well while the more heavily doped samples never have more than one. This result also indicates that screening of an electrostatic field at the surface is to a large extent determined by the Fermi energy of the bulk sample.

If we let the surface potential well assume the exponential form $U(z)=-U_0e^{-z/z_0}$, and let z_0 be the

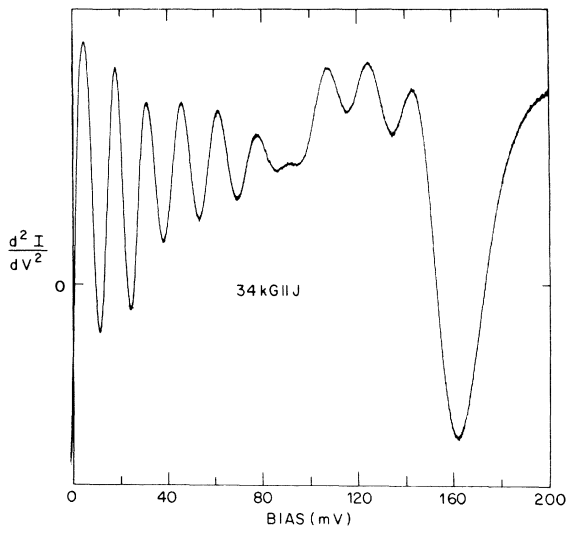

FIG. 6. Directly measured d^2I/dV^2-vs-V curve of sample 57894 in Table I. $T=4.2$ °K, $H=34$ kG. H is applied perpendicular to the junction surface.

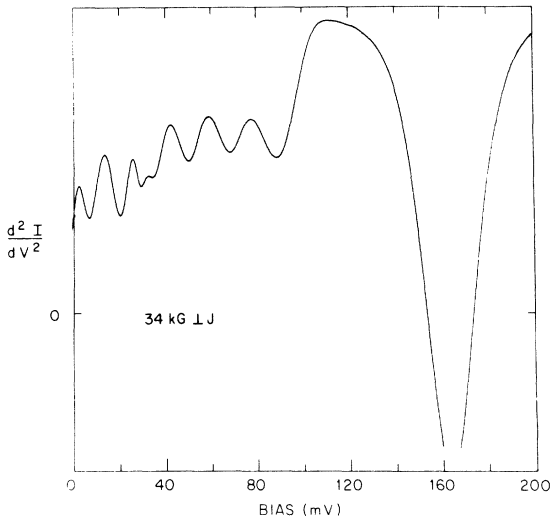

FIG. 7. Directly measured d^2I/dV^2-vs-V curve of sample 57894 in Table I. $T=4.2$ °K, $H=34$ kG. H is applied parallel to the junction surface.

Thomas-Fermi screening length of the bulk sample,[28] U_0 can be determined from the quantum level energy by using Eq. (5). For junction 311 of sample 5570, $z_0\approx100$ Å and the ground-state binding energy $E_{b1}=101$ mV. U_0 deduced from Eq. (5) is about 350 mV. However, this model potential also predicts a loosely bound ($E_{b2}\approx14$ meV) excited level which has not been observed. It may be suggested that the structure observed at the bias V_c, which reflects the conduction-band minimum, be attributed to this loosely bound level. Unfortunately, this interpretation does not agree with the observed Landau-level effects which will be discussed in Sec. IV B. We believe that the prediction of this additional bound level is an indication of the inadequacy of using this simple model potential to describe our results.

B. Landau Levels

When a magnetic field is applied perpendicular to the junction surface, two sets of oscillations have been observed in the tunneling curves of junctions fabricated on samples having $n\gtrsim1.5\times10^{17}/\mathrm{cm}^3$. For junctions fabricated on less heavily doped samples, we have observed three sets of oscillations. In each case, one set of oscillations arises from the Landau levels of the conduction-band electrons. This is established by the fact that this set of oscillations is observable when the magnetic field is oriented parallel to the surface while the other sets are not. This observation furnishes further evidence that there is only one quantized level in the surface potential well of the more heavily doped samples and that the structure observed at bias V_c reflects the conduction-band energy minimum.

Figure 6 shows the measured d^2I/dV^2-vs-V curve

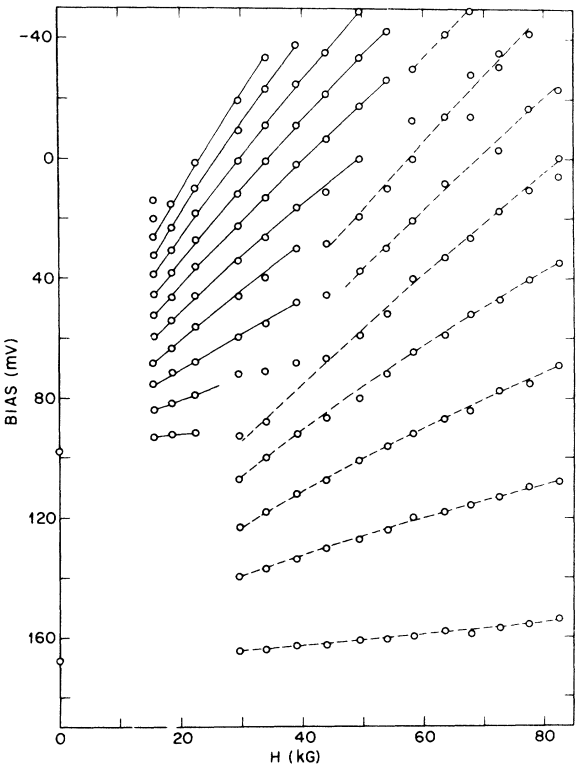

FIG. 8. Bias position, at which the oscillation minima in the d^2I/dV^2-vs-V curves are observed, plotted as a function of H for sample 57894. H is applied perpendicular to the junction surface.

of sample 57894 in Table I, while a magnetic field of 34 kG is applied perpendicular to the junction surface. The set, which is observable at $V \lesssim +100$ mV, is due to the Landau levels of the conduction band. We shall not discuss it further in this paper. The other set, which is observable at $V \lesssim +200$ mV, is due to the Landau levels of a two-dimensional subband. These oscillations correspond to about a 0.3% change of the junction conductance. It is shown in Fig. 7 that they disappear when the magnetic field is oriented parallel to the junction surface.

In Fig. 8, we plot the bias position of the oscillation dips observed in the d^2I/dV^2-vs-V curves as a function of the magnetic field H which is applied perpendicular to the surface. The data points group into two sets of curves. The set, which in the zero-field limit converges onto V_{b1} (168 mV), reflects the Landau-level spectra of the two-dimensional subband of the accumulation layer.

The period ΔV of the observed oscillations is equal to the Landau-level separation $\hbar\omega_c$. Hence the effective mass of the surface electrons can be deduced from $m^*/m = 2\mu_B H/e\,\Delta V$, where μ_B is a Bohr magneton. Figure 9 shows the surface electron effective mass determined in this way from the oscillations observed in the d^2I/dV^2- vs-V curves of this sample. If we neglect the effect of our applied bias on the subband energy, the quantity $e(V_{b1} - V)$ plotted as the horizontal axis is equal to the energy of the surface electron measured from the subband minimum. Then, the energy dependence of m^*/m shown here is a direct measure of the nonparabolicity of the subband energy structure.

However, when a positive bias is applied, it can increase the binding energy of the quantized level and bring the occupied Landau levels of the subband farther down below the Fermi level. The energy corresponding to the oscillation period ΔV, which is measured by applying a positive bias, will be larger than the Landau-level separation $\hbar\omega_c$ of the subband if there is no applied bias. As a result,

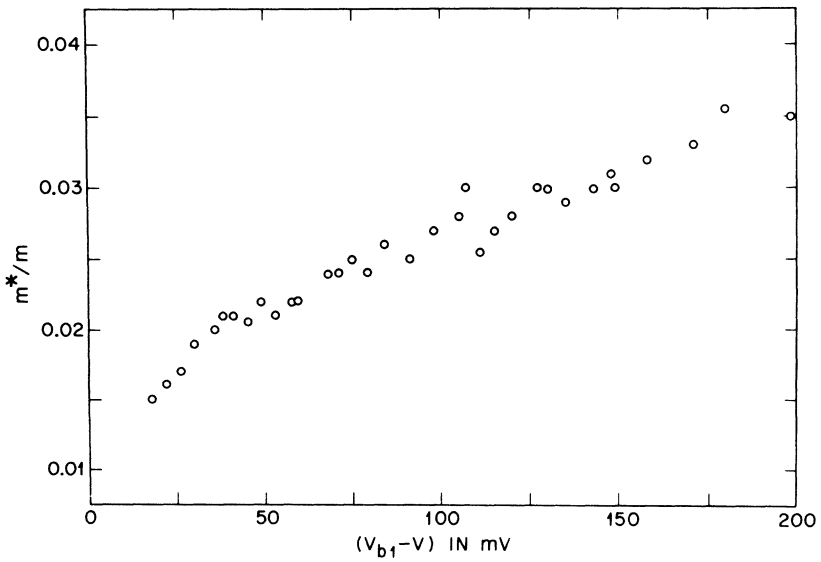

FIG. 9. Effective mass m^*/m of the surface electron determined from the period of the oscillations in the d^2I/dV^2-vs-V curves. $e(V_{b1} - V)$ is the energy of the surface electron measured from the subband minimum.

m^*/m obtained by measuring ΔV is reduced from its real value. Similarly, if a negative bias is applied, it reduces ΔV and increases m^*/m. This effect increases with increasing bias. Consequently, the electronic structure of the subband may be less nonparabolic than that shown by the bias dependence of m^*/m in Fig. 9 or the Landau-level spectra in Fig. 8. Unfortunately, we cannot estimate the magnitude of this effect at present. The data in Figs. 8 and 9 certainly show the upper limit of the nonparabolicity of the subband.

At a fixed magnetic field, the perpendicular component of the field, which determines the Landau-level separation,[3] can be varied by rotating the sample about an axis normal to the field direction. Figure 10 shows the orientation dependence of the subband Landau-level oscillations of this sample at 75 kG. The vertical axis is the bias position of the d^2I/dV^2 dips of the observed oscillations and θ is the angle between the field direction and the surface normal. It is obvious from the resulting Landau-level spectra that the Landau-level spacing depends only on the normal component of the applied field.

Figure 11 shows how the amplitude of the subband Landau-level oscillations, observed in the dI/dV-vs-V curves, depends on the perpendicular component of the applied magnetic field. The data are taken at a bias $V \approx +130$ mV. The crosses (×) are obtained by varying the magnetic field which is applied perpendicular to the surface, while the circles (○) are obtained by varying the sample orientation with the magnetic field fixed at 45 kG. The oscillation amplitude is measured accurate to ±1 of the units of the vertical scale; the orientation of the magnetic field relative to the sample normal is measured accurate to about ±3°. Within this experimental accuracy, the data points follow a straight line. This result indicates that the field dependence can be represented by an exponential form: $e^{-H_0/H}$. The parameter H_0 determined from the slope of the straight line is $H_0 = 130$ kG. We may also introduce an effective Dingle relaxation time[29] t_D by writing this oscillatory component of dI/dV as

$$(dI/dV)_{os} = C e^{-\pi/\omega_c t_D} \cos(2\pi e V/\hbar\omega_c + \varphi).$$

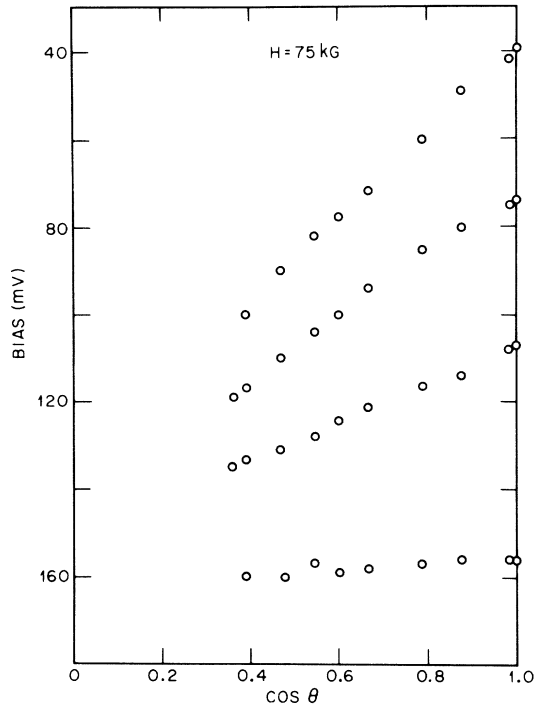

FIG. 10. Orientation dependence of the subband Landau-level oscillations of sample 57894 at $H = 75$ kG. The vertical axis is the bias position, at which the minima of the oscillations are observed in the d^2I/dV^2-vs-V curves. θ is the angle between the magnetic field direction and the surface normal.

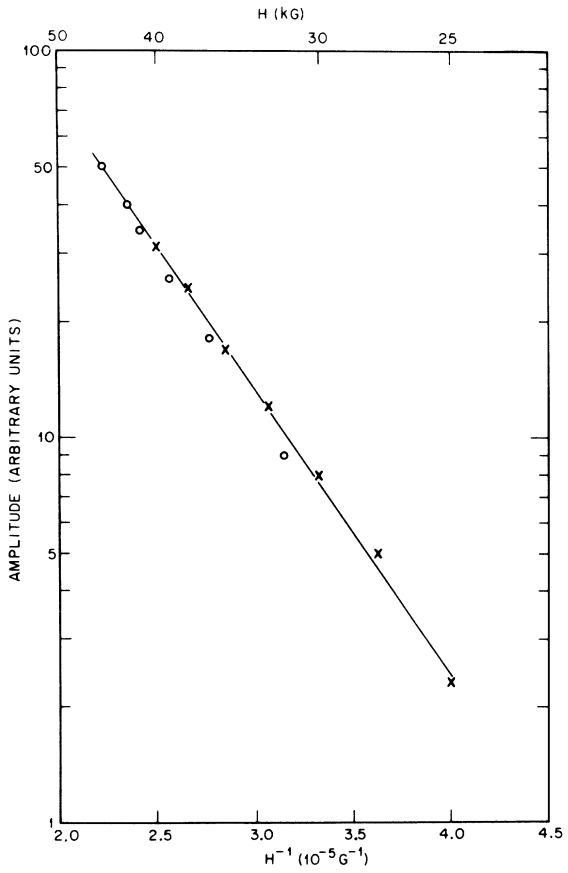

FIG. 11. Amplitude of the dI/dV oscillations at $V \approx +130$ mV as a function of the perpendicular component of the applied magnetic field. The crosses (×) are obtained by varying the magnetic field which is applied perpendicular to the surface. The circles (○) are obtained by varying the sample orientation with the magnetic field fixed at 45 kG.

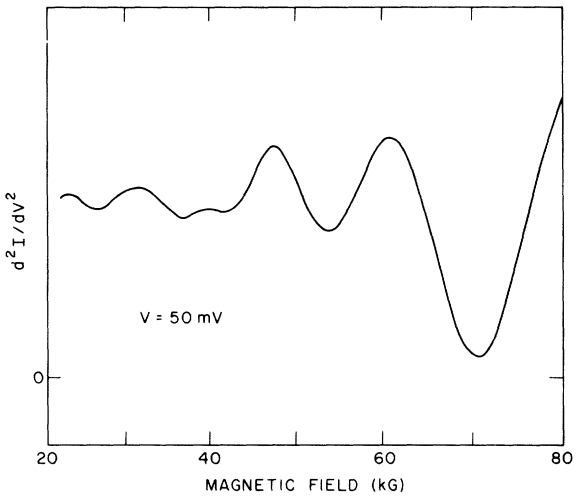

FIG. 12. Directly measured d^2I/dV^2-vs-H curve of sample 57894 at $V=+50$ mV. $T=4.2$ °K. H is applied perpendicular to the junction surface.

Here, C is a constant and φ is a phase angle. t_D is related to H_0 by $t_D=\pi m^*c/eH_0$. For $m^*=0.02m$, t_D deduced from the data given in Fig. 11 is 2.7×10^{-14} sec.

At a fixed bias V, if we vary the magnetic field, the surface electron density of states at an energy eV from the InAs Fermi level reaches a peak each time a Landau level coincides with this energy. This fluctuation in the density of states is reflected in the dI/dV- and d^2I/dV^2-vs-H curves as de Haas–van Alphen–type oscillations periodic in $1/H$. In Fig. 12, two sets of such oscillations are apparent in the d^2I/dV^2-vs-H curve of sample 57894 at $V=+50$ mV. The set, which is observable at $H\gtrsim40$ kG, is due to the subband Landau levels. The period $\Delta(1/H)$ of the oscillations is 4.9×10^{-6} G^{-1}.

If we assume that the applied magnetic field does not modify the surface potential well $U(z)$ appreciably, the period $\Delta(1/H)$ of the oscillations observed at zero bias, which is due to the subband Landau levels, is related to the k-space area enclosed by the Fermi-energy contour.[29] The electron density N_s in the surface accumulation layer, which is equal to the total number of states contained inside this constant-energy contour, can be determined from $\Delta(1/H)$ by

$$N_s=\frac{e/\pi\hbar c}{\Delta(1/H)}$$

For the sample 57894, $\Delta(1/H)$ at zero bias is 2.8×10^{-6} G^{-1}, which gives a value of 1.7×10^{12}/cm^2 for N_s. On the other hand, if we assume a constant density of states for the subband, N_s can also be determined from the Fermi energy of the accumulation layer by $N_s=(m^*/\pi\hbar^2)V_{b1}$. For $m^*=0.02m$, the measured V_{b1} gives $N_s=1.4\times10^{12}$/cm^2. The fact that we have neglected the nonparabolic nature of the subband can account for the difference between these two results.

We have shown in Sec. IV A that there are two subbands of surface electrons in the accumulation layer of samples having $N\lesssim1.5\times10^{17}$/cm^3. In the presence of a quantizing magnetic field, the oscillations due to the Landau levels of both subbands have been observed in their tunneling curves. However, the energy minima of the subbands and the resistance of the tunnel junctions exhibit anomalous magnetic field dependence.[30] We shall discuss the Landau levels of the two subbands together with this anomalous magnetic field effect in a separate article.

ACKNOWLEDGMENTS

I am most grateful to J. A. Appelbaum, G. A. Baraff, W. L. McMillan, and J. M. Rowell for many valuable discussions, and to L. N. Dunkleberger for his able assistance.

[1]J. R. Schrieffer, in *Semiconductor Surface Physics*, edited by R. H. Kingston (Pennsylvania U. P., Philadelphia, 1957), p. 55.

[2]A. B. Fowler, F. F. Fang, W. E. Howard, and P. J. Stiles, Phys. Rev. Letters 16, 901 (1966).

[3]F. F. Fang and P. J. Stiles, Phys. Rev. 174, 823 (1968).

[4]M. Kaplit and J. N. Zemel, Phys. Rev. Letters 21, 212 (1968).

[5]S. Kawaji and H. C. Gatos, Surface Sci. 7, 215 (1967).

[6]Y. Katayama, N. Kotera, and K. F. Komatsubara, in *Proceedings of the Tenth International Conference on the Physics of Semiconductors, Cambridge, Mass.*, 1970 (U. S. Atomic Energy Commission, Oak Ridge, Tenn., 1970), p. 464.

[7]G. A. Antcliffe, R. T. Bate, and R. A. Reynolds, in *Proceedings of the Conference on the Physics of Semimetals and Narrow Gap Semiconductors, Dallas*, 1970 (unpublished).

[8]A. F. Tasch, Jr., D. D. Buss, R. T. Bate, and B. H. Breazeale, in *Proceedings of the Tenth International Conference on the Physics of Semiconductors, Cambridge, Mass.*, 1970 (U. S. Atomic Energy Commission, Oak Ridge, Tenn., 1970), p. 458.

[9]D. C. Tsui, Phys. Rev. Letters 24, 303 (1970).

[10]C. A. Mead and W. G. Spitzer, Phys. Rev. Letters 10, 471 (1963).

[11]T. E. Fischer, F. G. Allen, and G. W. Gobeli, Phys. Rev. 163, 703 (1967).

[12]F. Stern and W. E. Howard, Phys. Rev. 163, 816 (1967).

[13]J. A. Appelbaum and G. A. Baraff, Phys. Rev. B 4, 1235 (1971); *ibid.* 4, 1246 (1971); and G. A. Baraff and J. A. Appelbaum, *ibid.* (to be published).

[14]C. R. Duke, Phys. Rev. 159, 632 (1967).

[15]D. J. BenDaniel and C. B. Duke, Phys. Rev. 160,

679 (1967).
[16]A classical electrostatic calculation of the electric field penetration into electrodes was first given by H. Y. Ku and P. G. Ullman, J. Appl. Phys. 35, 265 (1964); also J. G. Simmons, Brit. J. Appl. Phys. 18, 269 (1967).
[17]See, for example, A. Many, Y. Goldstein, and N. B. Grover, *Semiconductor Surfaces* (North-Holland, Amsterdam, 1965), p. 132.
[18]D. C. Tsui, Bull. Am. Phys. Soc. 16, 418 (1971); Solid State Commun. 9, 1789 (1971).
[19]I. Giaever and K. Mergerle, Phys. Rev. 122, 1101 (1961).
[20]W. L. McMillan and J. M. Rowell, in *Superconductivity*, edited by R. D. Parks (Dekker, New York, 1969), Chap. 11.
[21]D. E. Thomas and J. M. Rowell, Rev. Sci. Instr. 36, 1301 (1965).
[22]J. M. Rowell, W. L. McMillan, and W. L. Feldmann, Phys. Rev. 180, 658 (1969).
[23]F. S. L. Hsu and J. E. Kunzler, Rev. Sci. Instr. 34, 297 (1963).
[24]F. Matossi and F. Stern, Phys. Rev. 111, 472 (1958); C. R. Pidgeon, D. L. Mitchell, and R. N. Brown, *ibid.* 154, 737 (1967).
[25]D. C. Tsui, in *Proceedings of the Tenth International Conference on the Physics of Semiconductors, Cambridge, Mass.*, 1970 (U. S. Atomic Energy Commission, Oak Ridge, Tenn., 1970), p. 468.
[26]The agreement is poor in the case of the least heavily doped samples, for which the effect of impurity banding is important.
[27]The number of atoms per unit area in the three major symmetry planes of an InAs crystal is $n_s(\{110\}) = 4/\sqrt{2}\,a^2$, $n_s(\{111\}) = 4/\sqrt{3}\,a^2$, and $n_s(\{100\}) = 2/a^2$. Here a is the InAs lattice constant.
[28]In Ref. 9, the electron screening length λ was incorrectly estimated. According to the Thomas-Fermi model, λ for the two samples is 100 and 180 Å.
[29]L. M. Roth and P. N. Argyres, in *Semiconductors and Semimetals*, edited by R. K. Willardson and A. C. Beer (Academic, New York, 1966), Vol. I, Chap. 6.
[30]D. C. Tsui, Bull. Am. Phys. Soc. 16, 143 (1971).

PHYSICAL REVIEW B VOLUME 4, NUMBER 12 15 DECEMBER 1971

Donor-Electron Transitions between States Associated with the X_{1c} and X_{3c} Conduction-Band Minima in GaP

A. Onton
IBM Thomas J. Watson Research Center, Yorktown Heights, New York 10598
(Received 10 June 1971)

Transitions from the ground states of Si, Te, and S donors associated with the lowest X conduction band have been observed to excited donor states associated with the next-higher X conduction band as well as transitions into the higher band. The X_{3c}-X_{1c} interband energy is found to be 355 ± 3 meV with the conductivity effective mass in the higher band being $(0.14 \pm 0.02)m_0$.

We report here the observation in GaP at 5.5 °K of transitions from the ground states of Si, Te, and S donors associated with the lowest X conduction band to excited states associated with the next-higher X conduction band. We believe this is the first direct observation of impurity levels within the conduction-band continuum, and certainly the first time they have been seen directly with optical excitation. Moreover, the experiment provides an excellent value for the X_{3c}-X_{1c} conduction-band crystal-field splitting as well as an estimate of the higher X conduction-band effective mass.

The first observation of impurity-related energy levels within the continuum of a band was by Zwerdling *et al.*[1] for B and Al acceptors in the valence band of silicon. The transitions observed were from the ground state (with s-like envelope function) associated with the $p_{3/2}$ valence band to p-like excited states associated with the spin-orbit split-off $p_{1/2}$ valence band. Kosicki and Paul[2] presented evidence for the existence of donor levels associated with higher-lying conduction bands in hydrostatic pressure measurements on GaSb.

Infrared-absorption measurements on GaP in the 300–600-meV photon energy range have been made previously by Spitzer *et al.*,[3] Zallen,[4] Zallen and Paul,[5] Remenyuk *et al.*,[6,7] and Shmartsev *et al.*[8] The observed absorption has been attributed to X_{1c}-X_{3c} band-to-band and donor-to-X_{3c} conduction-band transitions. The k-space symmetry of the final state has been shown to be consistent with hydrostatic pressure data[4,5] as well as extrapolation from data in $GaAs_{1-x}P_x$.[9]

The results of the present infrared-transmission measurements on GaP are shown in Fig. 1 for four samples doped with various donor species. Plotted is the absorptoin coefficient as a function of incident photon energy. The spectra are characterized by a relatively sharp principal absorption peak followed by a broader band at higher energy. A schematic representation of the energy levels involved in these transitions is shown in Fig. 2. We assign the principal peak to the $1s \rightarrow 2p'_{\pm}$ transition (i.e., from the ground state associated with the lower conduction band to the $m = \pm 1$ sublevel of the hydrogenic $2p$ state associated with the